Long noncoding RNA LOC100507661 exhibits oncogenic activity in thyroid cancer

Daham Kim

Department of Medical Science

The Graduate School, Yonsei University

Long noncoding RNA LOC100507661 exhibits oncogenic activity in thyroid cancer

Directed by Professor Kyung-Sup Kim

The Doctoral Dissertation
submitted to the Department of Medical Science,
the Graduate School of Yonsei University
in partial fulfillment of the requirements for the degree of
Doctor of Philosophy of Medical Science

Daham Kim

December 2016

This certifies that the Doctoral Dissertation of Daham Kim is approved.

Thesis Supervisor : Kyung-Sup Kim

Thesis Committee Member#1 : Eun Jig Lee

Thesis Committee Member#2 : Young Suk Jo

Thesis Committee Member#3 : Myoung Hee Kim

Thesis Committee Member#4 : Sang Kil Lee

The Graduate School
Yonsei University

December 2016

ACKNOWLEDGEMENTS

I would like to express my gratitude and respect for those who helped me to complete my thesis. First of all, I am deeply indebted to my supervisor Professor Kyung-Sup Kim for his kind help, guidance, support and encouragement throughout my years at the graduate school. I wish to express my warm and sincere thanks to Professor Eun Jig Lee, Young Suk Jo, Myoung Hee Kim, and Sang Kil Lee for their encouragement and practical advice throughout my study. Their guidance not only improved my thesis but also will benefit my future work. I would like to thank my laboratory colleagues for their assorted efforts and supports. They always play for my side and strengthen my will to achieve my ambition. Finally, I especially want to thank my family for their loving support.

TABLE OF CONTENTS

LIST OF FIGURES

LIST OF TABLES

ABSTRACT

Long noncoding RNA LOC100507661 exhibits oncogenic activity in thyroid cancer

Daham Kim

Department of Medical Science
The Graduate School, Yonsei University

(Directed by Professor Kyung-Sup Kim)

Recent advances in next-generation sequencing have revealed a variety of long noncoding RNAs (lncRNAs). However, studies of lncRNAs are at a very early stage, our knowledge of the biological functions and clinical implications remains limited. To investigate the roles of lncRNAs in thyroid cancers, we verified 56 lncRNAs identified as potential cancer-promoting genes in a previous study that analyzed 2,394 tumor SNP arrays from 12 types of cancer. Based on verified sequence information in NCBI and Ensembl, we ultimately selected three candidate lncRNAs for detailed analysis. One of the candidates, LOC100507661, was strongly upregulated in thyroid cancer tissues relative to paired contralateral normal tissue. LOC100507661 was easily detectable in papillary and anaplastic thyroid cancer cell lines such as TPC1, BCPAP, C643, and 8505C, but not in the follicular thyroid cancer cell line FTC133. Stable overexpression of LOC100507661 promoted cell proliferation, migration, and invasion of thyroid cancer cells. Lymph node metastasis and BRAF V600E mutations were more frequent in

papillary thyroid cancers with high LOC100507661 expression. LOC100507661 expression was regulated by HER3 in thyroid cancer cell line. Our data demonstrate that LOC100507661 expression is elevated in human thyroid cancer and may play a critical role in thyroid carcinogenesis. Although more research is needed, the lncRNAs such as LOC100507661 can be a potential biomarker and therapeutic target in thyroid cancer.

Key words : long noncoding RNA, LOC100507661, thyroid cancer, carcinogenesis

Long noncoding RNA LOC100507661 exhibits oncogenic activity in thyroid cancer

Daham Kim

Department of Medical Science
The Graduate School, Yonsei University

(Directed by Professor Kyung-Sup Kim)

I. INTRODUCTION

Over 90% of the genome consists of noncoding RNAs (ncRNAs) that are transcribed but do not encode proteins.[1] These ncRNAs are divided into two major groups based on their size: small ncRNAs and long noncoding RNAs (lncRNAs). Small ncRNAs, which include transcripts such as ribosomal RNAs, transfer RNAs, micro RNAs, and small interfering RNAs, exhibit strong conservation across diverse species and their functions are relatively well known.[2] LncRNAs are defined as non-protein coding transcripts longer than 200 nucleotides. In contrast to small ncRNAs, lncRNAs are generally not strongly conserved, and their functions are much less well understood.[3] However, several recent studies revealed diverse roles of lncRNAs, including positive or negative effects on transcription and modulation of RNA processing or protein activity; moreover, some lncRNAs serve as precursors for smaller regulatory RNAs.[4] In addition, lncRNAs are receiving growing attention because they have important functions in

tumor biology.[5,6]

Although a few lncRNAs such as HOTAIR, H19, and MALAT1 have been investigated in the context of human cancers, fewer studies have focused specifically on the roles of lncRNAs in thyroid cancer.[7-11] Yoon et al. reported that NAMA (noncoding RNA associated with MAP kinase pathway and growth arrest), which promotes growth arrest, is downregulated in papillary thyroid carcinoma (PTC) harboring BRAF mutations.[12] Likewise, PTCSC1 (Papillary Thyroid Carcinoma Susceptibility Candidate 1) in 8q24, PTCSC2 in 9q22, and PTCSC3 in 14q13, which act as tumor suppressors, are downregulated in papillary thyroid carcinoma.[13-16] Conversely, BANCR (BRAF-activated lncRNA), which promotes cell proliferation and activates autophagy, is upregulated in PTC.[17]

Recent advances in next-generation sequencing have discovered various kinds of lncRNAs with potentially critical functions in carcinogenesis in a wide range of human cancers.[5] In this study, we sought to verify lncRNAs described in a previous study and to investigate the biological functions and clinical implications of lncRNAs with potentially important roles in thyroid carcinogenesis.

II. MATERIALS AND METHODS

1. Patients and samples

Samples of human thyroid cancer tissue and matched contralateral normal tissue were obtained from 64 patients who underwent thyroidectomy for PTC between April and November 2014 at Yonsei Cancer Center (Seoul, Korea). All samples were frozen in liquid nitrogen and stored at -80°C until use. Clinicopathological parameters were retrospectively collected from databases at our institutions. The study protocol was approved by our institutional review board, and informed consent was waived because of the retrospective nature of this study.

2. TCGA thyroid cancer data

The lncRNA, mRNA expression values, BRAF V600E mutation status and clinical information of thyroid cancer patients were downloaded from The Atlas of Noncoding RNAs in Cancer (TANRIC) and The Cancer Genome Atlas (TCGA).[18-20]

3. Reagents

U0126, and PD98059 were purchased from Cell Signaling Technology (MA, USA). SCH772984 and PLX4720 were purchased from Selleckchem (TX, USA). All drugs were dissolved in dimethyl sulfoxide (DMSO).

4. Cell culture

HEK293T, HEK293FT, FTC133, and TPC1 cells were cultured in Dulbecco's modified Eagle's medium, and BCPAP, C643, and 8505C cells were cultured in RPMI-1640 (Hyclone, UT, USA). Culture media were supplemented with 10% fetal bovine serum (FBS) and 1% penicillin/streptomycin. The cells were maintained in a humidified atmosphere of 5% CO2 and 95% air at 37°C.

5. RNA isolation and real-time PCR analysis

Total RNA was extracted from cell lines, thyroid cancer tissue, and matched contralateral normal tissue using the TRIzol® reagent (Invitrogen, MA, USA), and cDNA was synthesized from 2 μg of total RNA using the QuantiTect Reverse Transcription Kit (Qiagen, CA, USA). The following primers were used: 5'-CACTCCAAGTCCAGAGACCG-3' (sense) and 5'-CTAGGCTGCACCTCACCTTC-3' (antisense) for CTD-3080P12.3; 5'-AGAAACCTTCTGCCACCCAAA-3' (sense) and 5'-GCTGAACGCCCAATACAGGA-3' (antisense) for LOC100507661; 5'-ACCCTAACTGAGAAGGGCGT-3' (sense) and 5'-GGCCAGCAGCTGACATTTTT-3' (antisense) for TERC; 5'-GCTCTGTGGTGTGGGATTGA-3' (sense) and 5'-GTGGCAAAATGGCGGACTTT-3' (antisense) for MALAT1; 5'-GATGGGGAACCTTGAGATTG-3' (sense) and 5'-GGCAAACTTCCCATCGTAGA-3' (antisense) for HER3; and 5'-GGAGCGAGATCCCTCCAAAAT-3' (sense) and 5'-GGCTGTTGTCATACTTCTCATGG-3' (antisense) for GAPDH. Real-time PCR reactions consisted of 10 μl of Power SYBR® Green PCR Master Mix (Applied Biosystems, CA, USA), 5 pmol each of forward and reverse primers, 2 μl of diluted cDNA template, and sterile distilled water to a final volume of 20 μl. PCR was performed on an ABI StepOnePlus Real Time PCR system (Applied Biosystems, CA, USA) with the following conditions: 95°C for 10 min, followed by 40 cycles of 95°C for 15 sec and 60°C for 1 min. The comparative cycle threshold (CT) method was used to evaluate relative quantification. GAPDH was used as an internal control.

6. Small hairpin RNA (shRNA), GapmeR and small interfering RNA (siRNA) transfection

A set of four LOC100507661 shRNAs and a scrambled negative control were

purchased from OriGene (MD, USA). HEK293T cells were seeded into 6-well plates and transfected with 3 μg of shRNA using the JetPei transfection reagent (Polyplus, CA, USA). shRNA-transfected cells were subjected to real-time PCR analysis 48 hr after transfection.

The top three LOC100507661 GapmeRs ranked according to their design score and a negative control and a positive control (MALAT1) were purchased from EXIQON (MA, USA). 8505C cells were seeded into 6-well plates and transfected with GapmeR (final concentrations, 15 nM and 50 nM) using the Lipofectamine RNAiMAX Reagent (Invitrogen, CA, USA). GapmeR-transfected cells were subjected to real-time PCR analysis 48 hr after transfection.

The siRNA (small interfering RNA) sequences were as follows: BRAF siRNA sense 5'-CAGUUGUCUGGAUCCAUUUTT-3', antisense 5'-AAAUGGAUCCAGACAACUGTT-3'; HER3-1 siRNA sense 5'-ACGAUGGGAAGUUUGCCAUTT-3', antisense 5'-AUGGCAAACUUCCCAUCGUTT-3'; HER3-2 siRNA sense 5'-AGAACCAAUACCAGACACUTT-3', antisense 5'-AGUGUCUGGUAUUGGUUCUTT-3'; HER3-3 siRNA sense 5'-GCUCCGAUUGCAAUUUGCATT-3', antisense 5'-UGCAAAUUGCAAUCGGAGCTT-3'. BRAF siRNA was purchased from Ambion (TX, USA), and HER3 siRNAs were purchased from Bioneer (Seoul, Korea). The siRNAs were transfected into cells, which were cultured on six-well plates, using the Lipofectamine RNAiMAX Reagent (Invitrogen, CA, USA) according to the manufacturer's instructions.

7. LOC100507661 cloning and RNA labeling by MS2 tagging

The full-length cDNA of human LOC100507661 was amplified by performing RT-PCR on RNA extracted from thyroid cancer tissue harboring abundant LOC100507661, using primers 5'-CTCGGATCCTACCATCATGGCTCACTGC AACCTC-3' (sense) and 5'-CCCTCTAGCGGCCGCTTTTTATGCATCAAAAA

TAAAGGTG-3' (antisense) and inserted into the BamHI/NotI restriction sites of pcDNA3.1, yielding pcDNA-7661. To validate the lncRNA sequence, we cloned human LOC100507661 from three independent thyroid cancer samples. The analysis of sequences obtained using the ABI PRISM 3100 automated capillary DNA Sequencer (Applied Biosystems, CA, USA) did not show any differences in nucleotide sequence between the three plasmids.

For RNA labeling using MS2, pMS2-GFP was purchased from Addgene (a gift from Robert Singer, Addgene plasmid # 27121, MA, USA). Twenty-four copies of the MS2 stem-loop were amplified from pCR4-24XMS2SL-stable (Addgene plasmid # 31865) and inserted at the 3' end of LOC100507661 in pcDNA-7661, yielding pcDNA-7661-24XMS2SL construct. TPC1 and 8505C cells were cotransfected with pMS2-GFP and pcDNA-7661-24XMS2SL. After 24 hr, one drop of Vectashield Hard Set Mounting Medium with DAPI (H-1500, Vector Laboratories, CA, USA) was added, and images were acquired on a ZEN2012 laser scanning system (Carl Zeiss, Oberkochen, Germany) controlled by the LSM 700 software (Carl Zeiss) as described.[21]

8. Construction and use of a lentiviral vector expressing LOC100507661

The LOC100507661 region of pcDNA-7661 was inserted into the lentiviral vector pLECE3 using BamHI/NotI restriction sites to make pLECE3-7661. pLECE3 was a kind gift from Dr. KH Chun.[22] Lentiviral particles were generated using three plasmids, VSVG, RSV-REV, and PMDLg/pPRE, in HEK293FT cells cotransfected with pLECE3. Cells were transfected using the JetPei transfection reagent. Two days after transfection, culture media were passed through a 0.45 μm filter and the purified lentiviral particles were used to infect thyroid cancer cell lines.

9. pCMV-MEK1-DD plasmid transfection

The pCMV-Myc-MEK1_218D222D (pCMV-MEK1-DD) was a kind gift from

Dr. Hyungjin Rhee. The plasmid were transfected into cells, which were cultured on six-well plates, using the Lipofectamine 3000 Reagent (Invitrogen, CA, USA) according to the manufacturer's instructions.

10. Cell proliferation assay

Cell proliferation was determined using the WST colorimetric assay (EZ-CyTox, Daeil Lab Service, Seoul, Korea). In 96-well plates, 5×10^3 cells/well were seeded and incubated for 24 hr. After addition of 10 μl of WST reagent to each well, the plate was incubated for 2 hr, and absorbance was detected at a wavelength of 450 nm. The assay was performed in triplicate. Cell numbers were determined using the EVE™ automatic cell counter (NanoEntek, Seoul, Korea).

11. Wound-healing/migration assay

Cells were seeded in 6-well culture plates and allowed to form a confluent monolayer. A scratch wound was induced with a 1000 μl pipette tip. To remove debris, cells were washed with PBS, and replaced media. Images were obtained at 0 and 24 hr after scratching. The size of the wound was measured using Image J software. Data are shown as a percentage of the control. The assay was performed in triplicate.

12. Matrigel invasion assay

Cells were seeded (2.5×10^4 cells in 0.5 ml of media lacking FBS) into 24-well Matrigel Invasion Chambers (Corning, NY, USA) with polyethylene terephthalate membrane containing 8.0 μm pores. As a chemotaxis factor, FBS (10%) was added to the lower compartment of the chambers. After incubation for 24 hr at 37°C, all cells that did not enter the filter were removed by gently scraping the upper side of the filter with a wet cotton swab. Cells that migrated to the bottom filter surface were fixed by soaking the insert in MeOH for 3 min, stained with hematoxylin and eosin, and air-dried. Filters cut from inserts were mounted

upside-down on glass slides. Invading cells were counted under a light microscope. The assay was performed in triplicate.

13. Western blotting

Total proteins were extracted from cells by using the Cell Extraction Buffer (Invitrogen, CA, USA). Protein concentration was measured using the BCA Protein Assay Kit (Thermo Scientific, IL, USA). Equal amounts of total protein lysate were separated by 10% SDS-PAGE and transferred onto PVDF membranes. After blocking in 5% skim milk, the membranes were probed with targeted primary antibodies overnight at 4°C and detected by incubating with specific secondary antibodies for 1 hr at room temperature. Signals were detected using a West Save Up immunoblotting detection kit (Ab Frontier, Seoul, Korea). Antibodies against HER3, pERK, ERK, pAKT, and AKT were purchased from Cell Signaling Technology (MA, USA). Antibodies against BRAF and B-actin were purchased from Santa Cruz biotechnology (CA, USA). B-actin was used as a loading control.

14. Statistical Analysis

SPSS Statistics Version 21 (IBM, NY, USA) was used for all statistical analyses. All results are expressed as means ± SD or means ± SEM. Statistical comparisons of mean values were performed using the Mann–Whitney U-test or Student's t-test, and group comparisons were performed by $\chi 2$ test or linear by linear association, as appropriate.

III. RESULTS

1. Identification of lncRNA genes with oncogenic activity in thyroid cancer

To verify newly discovered lncRNAs, we reviewed the results of a previous study that analyzed 2,394 tumor SNP arrays from 12 types of cancer in the Tumorscape database created by the Broad Institute.[23] A total of 1,064 lncRNAs were located in 76 regions with focal positive somatic copy number alterations (SCNAs) (i.e., gains in copy number). The top 20 most significant focal alteration peaks contained 56 lncRNAs. We reasoned that lncRNAs in regions with a higher frequency of genomic alterations were more likely to contribute to carcinogenesis and/or cancer progression. Because very little information is available about lncRNAs, we chose candidate genes based on the availability of genome annotations in both NCBI and Ensembl, and excluded partially located genes, pseudogenes, non-validated genes, long transcripts over 2000 bp, and genes that have known variants. Ultimately, we selected three candidate genes (CTD-3080P12.3, LOC100507661, and TERC) for further analysis (Fig. 1A).

Initially, we used real-time PCR to compare the expression patterns of these three candidate lncRNAs in thyroid cancer tissue and matched contralateral normal tissue from six randomly selected patients (Fig. 1B). CTD-3080P12.3 exhibited no specific pattern, and TERC was downregulated, in thyroid cancer tissue. By contrast, LOC100507661 was strongly upregulated in thyroid cancer tissue relative to control tissue. Therefore, we decided to study this lncRNA in detail.

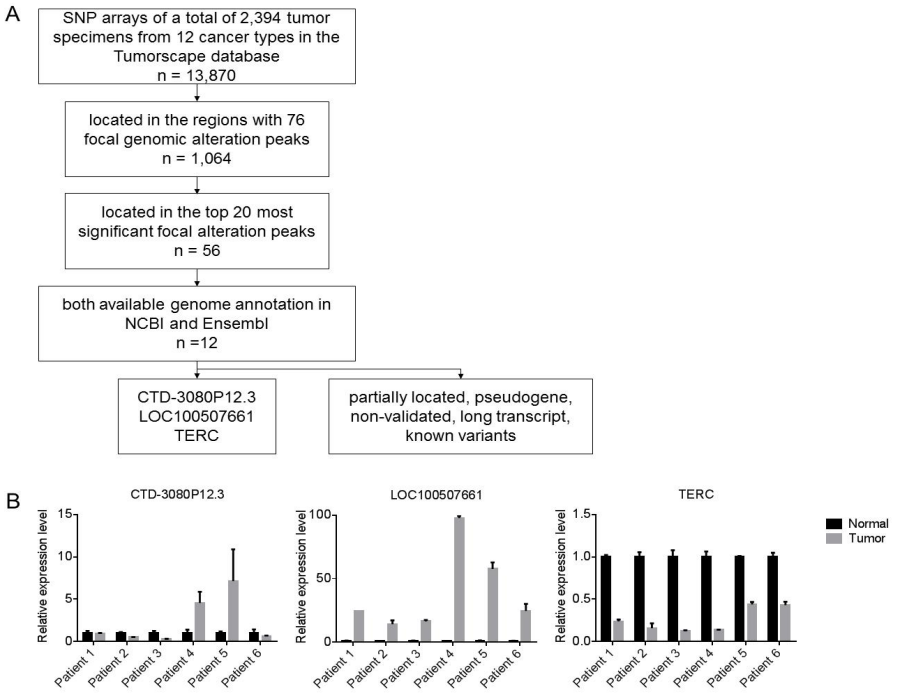

Figure 1. Identification of lncRNA genes with oncogenic activity in thyroid cancer. (A) Flowchart for identification of lncRNA genes with oncogenic activity. (B) Representative results of real-time PCR for three candidate lncRNAs. GAPDH was used as an internal control.

2. Characteristics of LOC100507661

LOC100507661, which is localized on human chromosome 3 (q26.2), is a 745 bp transcript consisting of five exons (Fig. 2A). We predicted LOC100507661 secondary structure (Fig. 2B) using the CENTROIDFOLD web server (http://www.ncrna.org/centroidfold/), a web application for RNA secondary structure prediction powered by one of the most accurate prediction engines.[24] The functions of lncRNAs are dictated by their secondary structures rather than by their primary sequences.[25] Notably, part of exon 1 is the reverse complement of the anterior portion of exon 2. The base-pairing probability of this region is very high, and the resultant structure may be related to the function or stability of the molecule (indicated by red color in Fig. 2B).

Although little is known about LOC100507661, its tissue-specific expression patterns are available at BIOGPS (http://biogps.org) (Fig. 2C). LOC100507661 is expressed at a lower level in thyroid (6.05) than in other tissues (mean, 6.16), but at a higher level in fetal thyroid (6.4). These data are consistent with the idea that LOC100507661 plays a role in thyroid development and carcinogenesis.

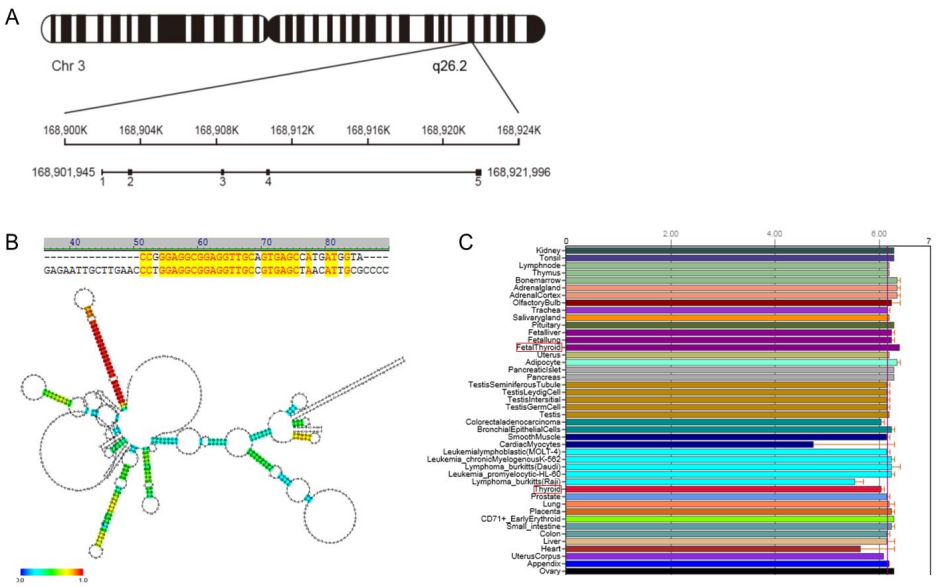

Figure 2. Characteristics of LOC100507661. (A) Genomic location of LOC100507661. (B) Predicted structure of LOC100507661 by CENTROIDFOLD. Upper line: reverse complement of exon 1; lower line: anterior portion of exon 2. (C) Tissue-specific expression patterns of LOC100507661 at BIOGPS.

3. Levels of LOC100507661 in thyroid cancer cell lines

Next, we analyzed the expression of LOC100507661 in thyroid cancer cell lines (Fig. 3A, 3B). This lncRNA could be detected in PTC cell lines such as TPC1 and BCPAP, but was barely detectable in the follicular thyroid cancer (FTC) cell line FTC133. Expression was higher in anaplastic thyroid cancer (ATC) cell lines such as C643 and 8505C. In addition, levels were higher in cell lines harboring BRAF V600E mutations (8505C vs C643 and BCPAP vs TPC1). These results suggest that LOC100507661 is associated with aggressive tumor behavior in thyroid cancer, and that BRAF signaling may have positive relationships with LOC100507661.

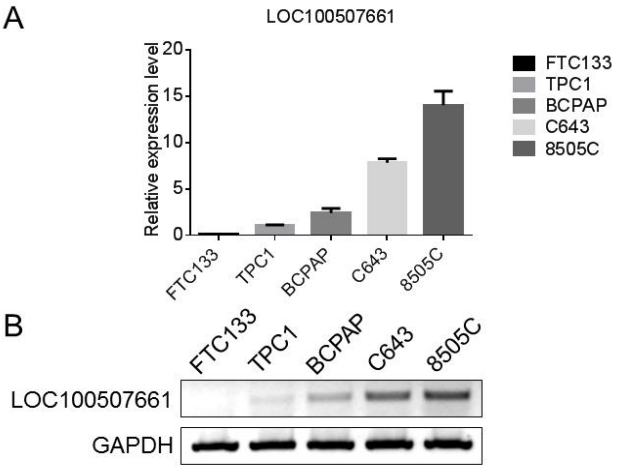

Figure 3. LOC100507661 levels in thyroid cancer cell lines. (A, B) Levels of LOC100507661 in thyroid cancer cell lines, determined by real-time PCR and RT-PCR.

4. Transfection of cell lines with LOC100507661 shRNA and GapmeR

To investigate the potential biological function of LOC100507661, we attempted to knockdown LOC100507661 using shRNA. To this end, we transfected HEK293T cells with a set of four LOC100507661 shRNAs or a scrambled negative control; this cell line was selected because of its high transfection efficiency. Unfortunately, although 70–80% transfection efficiency was achieved (as determined by GFP expression; data not shown), this set of constructs failed to knockdown gene expression (Fig. 4A). A second set of constructs also failed to achieve knockdown (Fig. 4B). We postulated that the subcellular localization of this lncRNA might affect the efficiency of shRNA-mediated knockdown.

To characterize the localization of LOC100507661, we labeled LOC100507661 RNA by MS2 tagging in TPC1 and 8505c cells.[21] The results revealed that LOC100507661 was exclusively localized to the nucleus, where shRNAs cannot promote the degradation of target RNAs (Fig. 4C).

Next, we transfected 8505C cells with LOC100507661 GapmeRs or a negative control or a positive control (MALAT1). The positive control (MALAT1) achieved significant knockdown. However, LOC100507661 GapmeRs did not achieve sufficient knockdown (Fig. 4D). The secondary structure of the lncRNA or an unknown mechanism might prevent GapmeR from accessing the target region.

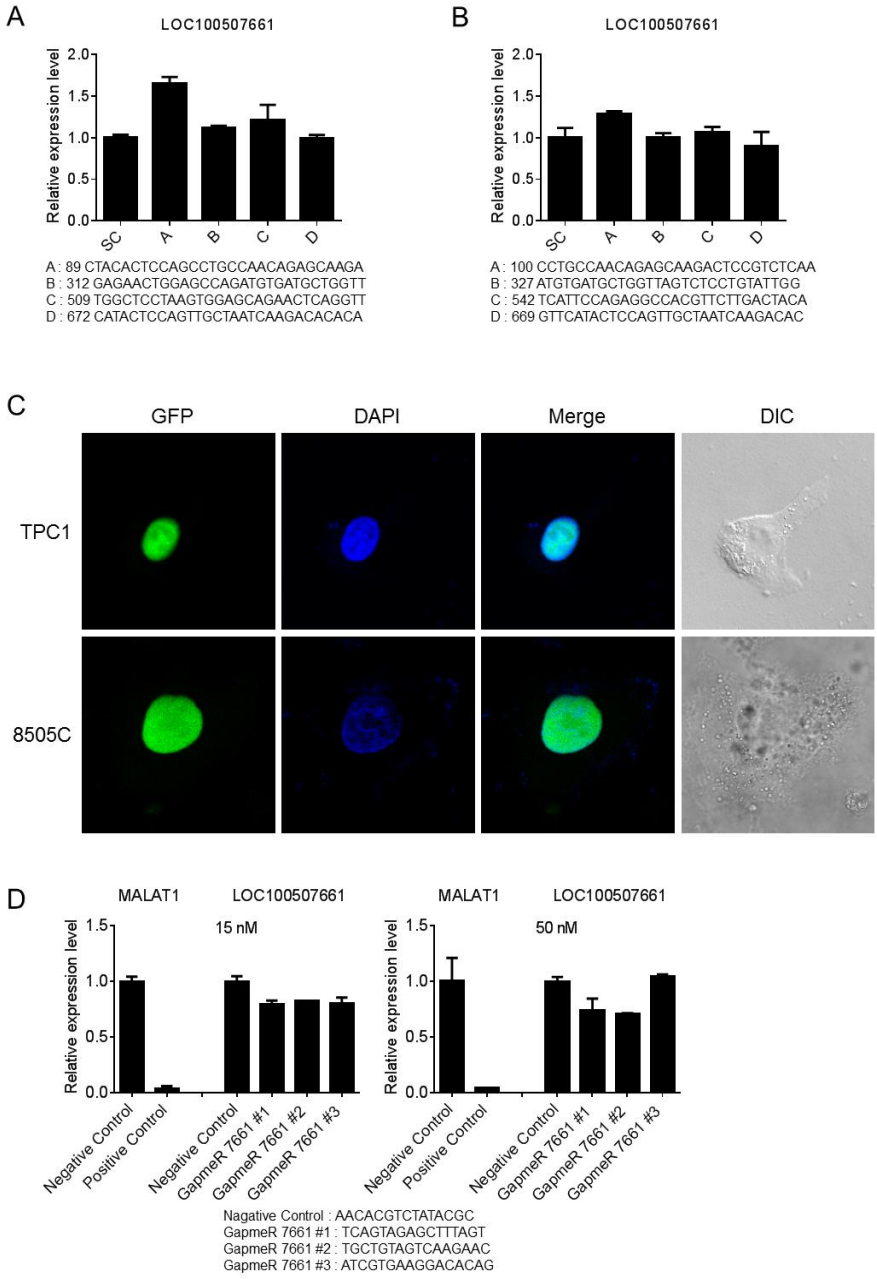

Figure 4. Transfection of cell lines with LOC100507661 shRNA and GapmeR. (A, B) Levels of LOC100507661 in HEK293T cells, determined by real-time PCR analysis 48 hr after shRNA transfection. (C) TPC1 and 8505C

cells were cotransfected with pMS2-GFP and pcDNA-7661-24XMS2SL plasmids. (D) Levels of MALAT1 (Positive Control) and LOC100507661 in 8505C cells, determined by real-time PCR analysis 48 hr after GapmeRs transfection.

5. Overexpression of LOC100507661 in thyroid cancer cells increases cell proliferation, migration, and invasion

To study the potential biological functions of LOC100507661 in thyroid cancer, we used a lentivirus (vector pLECE3) containing a LOC100507661 expression cassette driven by the CMV promoter (pLECE3-7661) to stably upregulate LOC100507661 expression. LOC100507661 expression levels were lower in TPC1 cells than in other PTC or ATC cell lines (Fig. 3A, 3B). Therefore, we used TPC1 cells for stable overexpression of LOC100507661 (Fig. 5A).

To determine the effect of LOC100507661 on proliferation, the stably overexpressing cells were subjected to WST colorimetric assay and cell counting (Fig. 5B, 5C). As expected, stable overexpression of LOC100507661 (SO7661) promoted cell proliferation of thyroid cancer cells. Next, we performed a wound-healing assay to test the effect of SO7661 on migration. Twenty-four hours after a monolayer was scratched, the size of the wound was smaller in TPC1 cells with SO7661 (Fig. 5D), indicating that LOC100507661 promotes the migration of thyroid cancer cells. In a Matrigel invasion assay, SO7661 increased invasion by TPC1 cells (Fig. 5E).

To verify the TPC1 data, we also used 8505C cells to obtain stable overexpression of LOC100507661 (Fig. 5F). SO7661 also promoted cell proliferation, migration and invasion of 8505C cells. (Fig. 5G, 5H, 5I, 5J). Together, these findings indicate that LOC100507661 can promote cell proliferation, migration, and invasion of thyroid cancer cells in vitro.

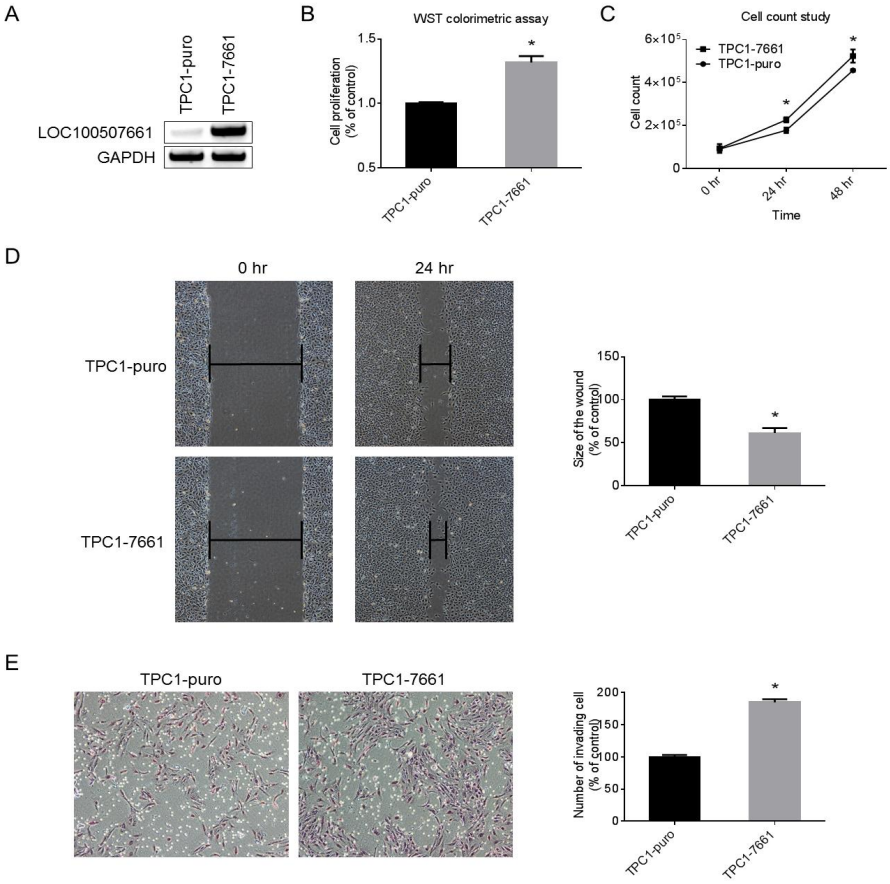

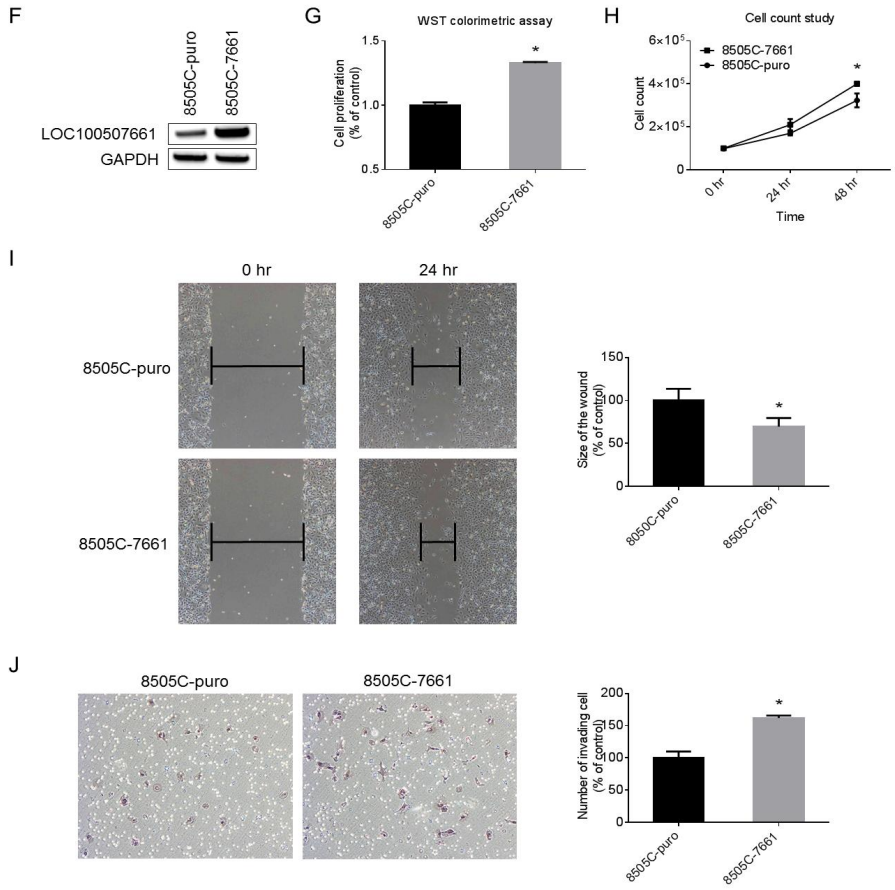

Figure 5. Overexpression of LOC100507661 in thyroid cancer cell lines. (A) LOC100507661 expression analyzed by RT-PCR in control TPC1 cells (TPC1-puro) and TPC1 cells stably overexpressing LOC100507661 (TPC1-7661). (B, C) Cell proliferation assays using TPC1-puro and TPC1-7661 cells. WST colorimetric assay (B) and cell counting (C). (D) Representative figures (left panel) and quantitative analyses (right panel) of TPC1-puro and TPC1-7661 cells (magnification, 40×) using the wound-healing/migration assay. (E) Representative figures (left panel) and quantitative analyses (right panel) of TPC1-puro and TPC1-7661 (magnification, 100×) using the Matrigel invasion assay. (F) Analysis of LOC100507661 expression by RT-PCR in 8505C-puro and 8505C-7661 cells. (G, H) Analysis of 8505C-puro and 8505C-7661 cell

proliferation using the WST colorimetric assay (G) and cell counting (H). (I) Representative figures (left panel) and quantitative analyses (right panel) of 8505C-puro and 8505C-7661 cells (magnification, 40×) using the wound-healing/migration assay (J) Representative figures (left panel) and quantitative analyses (right panel) of 8505C-puro and 8505C-7661 cells (magnification, 100×) using the Matrigel invasion assay. Data are expressed as means ± SD. *, $P < 0.05$.

6. LOC100507661 levels in thyroid cancer tissues

We examined the expression levels of LOC100507661 from 64 patients (Fig. 6A, 6B). Almost all (60/64, 93.8%) had higher levels of LOC100507661 in thyroid cancer tissue than in matched contralateral normal tissue, confirming that LOC100507661 levels are significantly upregulated in thyroid cancer tissue ($P = 0.0011$). These results are supported by LOC100507661 RPKM expression data from the TCGA thyroid cancer database (Fig. 7A). Consistent with this, datasets from thyroid cancer, hepatoblastoma, and hepatocellular carcinoma recently deposited in GEO (Gene Expression Omnibus) also revealed statistically significant upregulation of LOC100507661 in multiple cancers (Fig. 7B). Interestingly, the expression levels of LOC100507661 were much higher in metastatic lymph nodes than in normal thyroid tissue (Fig. 6C), suggesting that LOC100507661 might play a role in lymph node metastasis.[26]

As the FTC cell line showed lower LOC100507661 expression than the PTC or ATC cell line, we compared the expression levels between FTC, follicular variant, and classical PTC samples using real-time PCR (Fig. 6D). The results showed the expression level of LOC100507661 was not increased in the FTC and was much lower in the follicular variant type than in the classical type. To validate our result, we analyzed the TCGA thyroid cancer database, and compared the expression levels of LOC100507661 between follicular variant PTC and classical PTC. Interestingly, the expression levels of LOC100507661 were significantly lower in the follicular variant type (0.32 ± 0.55, $N = 101$) than in the classical type (0.54 ± 0.44, $N = 349$), ($P<0.001$).

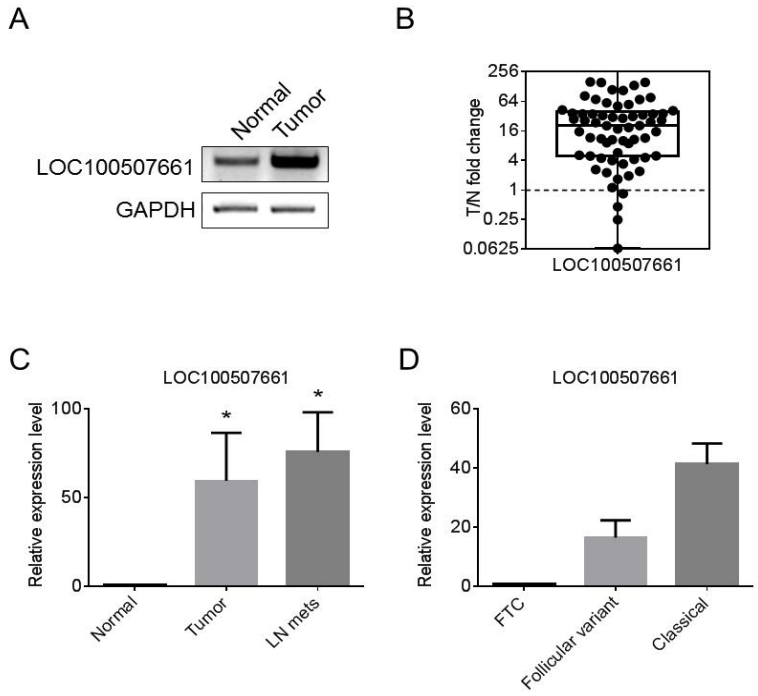

Figure 6. Levels of LOC100507661 in thyroid cancer tissues. (A) Representative RT-PCR of thyroid cancer tissue and matched contralateral normal tissue. (B) LOC100507661 fold changes in thyroid cancer tissue relative to matched contralateral normal tissue, determined by real-time PCR (N = 64). (C) LOC100507661 levels in samples with metastatic lymph node pairs. Data are expressed as means ± SEM. *, $P < 0.05$ versus Normal (N = 5). (D) LOC100507661 levels in FTC, follicular variant, and classical PTC. Data are expressed as means ± SEM.

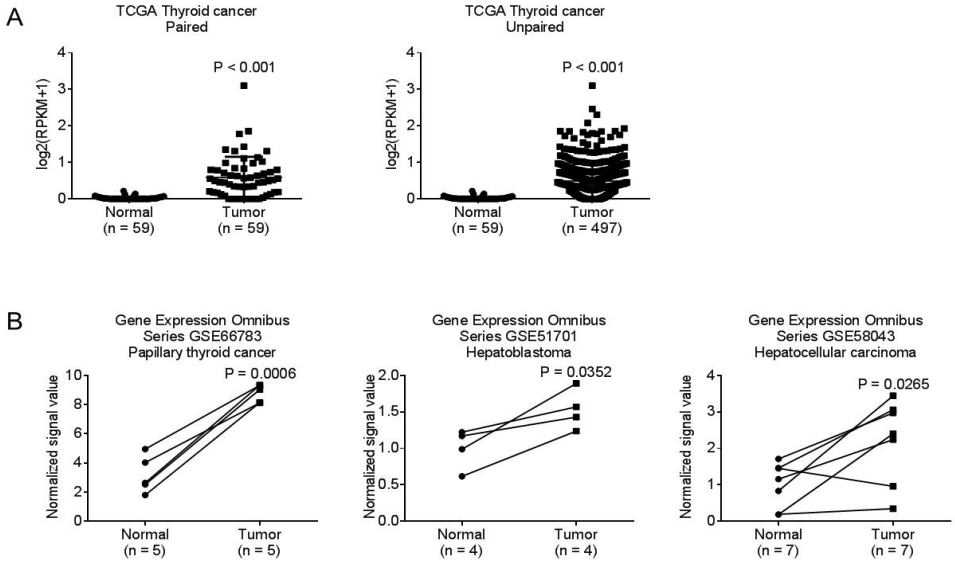

Figure 7. Levels of LOC100507661 in other data. (A) LOC100507661 RPKM expression data from the TCGA thyroid cancer database. RPKM values are expressed as log2(RPKM+1) because they are log-normally distributed. (B) LOC100507661 expression in datasets from thyroid cancer, hepatoblastoma, and hepatocellular carcinoma deposited in GEO.

7. Clinicopathological characteristics of patients with thyroid cancer according to LOC100507661 expression status in our study patients

According to the median level of LOC100507661, we divided patients into two groups, reduced or moderately elevated expression (N = 32) and highly elevated expression (N = 32), and compared their clinicopathologic characteristics (Table 1). The analysis showed that high LOC100507661 expression in thyroid cancer was associated with lymph node metastasis (P = 0.035) and BRAF V600E mutations (P = 0.016), but not with other parameters such as age (P = 0.297) and gender (P = 0.140). Univariate analysis (Table 2, Table 3) and multivariate analysis confirmed that high LOC100507661 expression was associated with lymph node metastasis (Table 4) and BRAF V600E mutations (Table 5).

Table 1. Clinicopathological characteristics of patients with thyroid cancer according to LOC100507661 expression status in our study patients

	LOC100507661 Expression		P-value
	Reduced or moderately elevated (N = 32), n (%)	Highly elevated (N = 32), n (%)	
LOC100507661	7.49 ± 6.11	63.78 ± 47.92	<0.001*
Age (yr), mean ± SD	42.6 ± 16.7	38.5 ± 14.4	0.297*
Gender (F/M)			
Male	10 (31.3)	5 (15.6)	0.140†
Female	22 (68.8)	27 (84.4)	
Tumor size (cm)	2.4 ± 0.9	2.6 ± 2.1	0.676*
Extrathyroidal extension			
Negative	7 (21.9)	6 (18.8)	0.756†
Positive	25 (78.1)	26 (81.3)	
Multifocality			
Negative	17 (53.1)	12 (37.5)	0.209†
Positive	15 (46.9)	20 (62.5)	
T-stage			
T1	5 (15.6)	5 (15.6)	0.558†
T2	2 (6.3)	1 (3.1)	
T3	23 (71.9)	21 (65.6)	
T4	2 (6.3)	5 (15.6)	
Regional lymph node			
N0	15 (46.9)	7 (21.9)	0.035†
N1	17 (53.1)	25 (78.1)	
Distant metastasis			
M0	31 (96.9)	30 (93.8)	0.554†
M1	1 (3.1)	2 (6.3)	
TNM stage group			
I	18 (56.3)	21 (65.6)	0.754†
II	1 (3.1)	2 (6.3)	
III	10 (31.3)	2 (6.3)	
IV	3 (9.4)	7 (21.9)	
BRAF V600E mutation			
Absent	11 (34.4)	3 (9.4)	0.016†
Present	21 (65.6)	29 (90.6)	

* P-values were calculated by Student's t-test. Data are expressed as means ± SD.

† P-values calculated by χ^2 test or linear-by-linear association.

Table 2. Univariate analysis of clinicopathological parameters and LOC100507661 expression according to the presence or absence of lymph node metastasis in our study patients

	Lymph node metastasis		P-value
	Absent (N = 22), n (%)	Present (N = 42), n (%)	
LOC100507661 group			
< median level	15 (68.2)	17 (40.5)	0.035†
≥ median level	7 (31.8)	25 (59.5)	
Age (yr), mean ± SD	46.0 ± 15.3	37.7 ± 15.2	0.045*
Gender (F/M)			
Male	5 (22.7)	10 (23.8)	0.923†
Female	17 (77.3)	32 (76.2)	
Tumor size (cm)	2.3 ± 0.9	2.6 ± 1.9	0.621*
Extrathyroidal extension			
Negative	9 (40.9)	4 (9.5)	0.003†
Positive	13 (59.1)	38 (90.5)	
Multifocality			
Negative	12 (54.5)	17 (40.5)	0.283†
Positive	10 (45.5)	25 (59.5)	
T-stage			
T1	7 (31.8)	3 (7.1)	0.009†
T2	2 (9.1)	1 (2.4)	
T3	11 (50.0)	33 (78.6)	
T4	2 (9.1)	5 (11.9)	
Distant metastasis			
M0	22 (100.0)	39 (92.9)	0.199†
M1	0 (0.0)	3 (7.1)	
TNM stage group			
I	14 (63.6)	25 (59.5)	0.568†
II	0 (0.0)	3 (7.1)	
III	7 (31.8)	5 (11.9)	
IV	1 (4.5)	9 (21.4)	
BRAF V600E mutation			
Absent	5 (22.7)	9 (21.4)	0.905†
Present	17 (77.3)	33 (78.6)	

* P-values were calculated by Student's t-test. Data are expressed as means ± SD.

† P-values calculated by χ^2 test or linear-by-linear association.

Table 3. Univariate analysis of clinicopathological parameters and LOC100507661 expression according to the presence or absence of BRAF V600E mutation in our study patients

	BRAF V600E mutation		P-value
	Absent (N =14), n (%)	Present (N = 50), n (%)	
LOC100507661 group			
< median level	11 (78.6)	21 (42.0)	0.016†
≥ median level	3 (21.4)	29 (58.0)	
Age (yr), mean ± SD	35.5 ± 15.4	42.0 ± 15.5	0.170*
Gender (F/M)			
Male	3 (21.4)	12 (24.0)	0.841†
Female	11 (78.6)	38 (76.0)	
Tumor size (cm)	2.7 ± 0.9	2.4 ± 1.8	0.582*
Extrathyroidal extension			
Negative	4 (28.6)	9 (18.0)	0.385†
Positive	10 (71.4)	41 (82.0)	
Multifocality			
Negative	8 (57.1)	21 (42.0)	0.314†
Positive	6 (42.9)	29 (58.0)	
T-stage			
T1	3 (21.4)	7 (14.0)	0.376†
T2	1 (7.1)	2 (4.0)	
T3	9 (64.3)	35 (70.0)	
T4	1 (7.1)	6 (12.0)	
Regional lymph node			
N0	5 (35.7)	17 (34.0)	0.905†
N1	9 (64.3)	33 (66.0)	
Distant metastasis			
M0	13 (92.9)	48 (96.0)	0.623†
M1	1 (7.1)	2 (4.0)	
TNM stage group			
I	9 (64.3)	30 (60.0)	0.381†
II	1 (7.1)	2 (4.0)	
III	4 (28.6)	8 (16.0)	
IV	0 (0.0)	10 (20.0)	

* P-values were calculated by Student's t-test. Data are expressed as means ± SD.

† P-values calculated by χ^2 test or linear-by-linear association.

Table 4. Multivariate analysis of the association between lymph node metastasis and highly elevated LOC100507661 expression in our study patients

Highly elevated LOC100507661	Lymph node metastasis		
	Odds ratio	95% CI	P-value
Model 1	3.360	1.044–10.810	0.042
Model 2	5.336	1.211–23.517	0.027

Model 1. Adjusted for age and gender.

Model 2. Adjusted for age, gender, tumor size, extrathyroidal extension, multifocality, and BRAF V600E mutation.

Abbreviation: CI, confidence interval.

Table 5. Multivariate analysis of the association between the BRAF V600E mutation and highly elevated LOC100507661 expression in our study patients

Highly elevated LOC100507661	BRAF V600E mutation		
	Odds ratio	95% CI	P-value
Model 1	6.261	1.457–26.907	0.014
Model 2	7.587	1.536–37.475	0.013

Model 1. Adjusted for age and gender.

Model 2. Adjusted for age, gender, tumor size, extrathyroidal extension, multifocality, and lymph node metastasis.

Abbreviation: CI, confidence interval.

8. TCGA thyroid cancer data according to LOC100507661 expression status

The patients from the TCGA thyroid cancer database were also divided into low and high LOC100507661 expression groups according to the median level of LOC100507661 (Table 6). Consistent with our study patients data, high LOC100507661 expression was associated with lymph node metastasis ($P < 0.001$) and the BRAF V600E mutations ($P < 0.001$). The thyroid differentiation score (TDS) was negatively associated with high LOC100507661 expression.[18] Univariate analysis (Table 7, Table 8) and multivariate analysis also confirmed that high LOC100507661 expression was associated with lymph node metastasis (Table 9) and the BRAF V600E mutations (Table 10). Consistent with the data from our cell-based assays and real-time PCR on metastatic lymph nodes, these results imply that high LOC100507661 levels play important roles in tumor behavior and aggressiveness of thyroid cancer.

Table 6. Clinicopathological characteristics of patients with thyroid cancer according to LOC100507661 expression status from the TCGA thyroid cancer database

	LOC100507661 Expression		P-value
	Low group (N = 246), n (%)	High group (N = 247), n (%)	
LOC100507661	0.14 ± 0.13	0.84 ± 0.42	<0.001*
Age (yr), mean ± SD	49.2 ± 16.3	45.1 ± 15.0	0.004*
Gender (F/M)			
Male	63 (25.6)	70 (28.3)	0.495†
Female	183 (74.4)	177 (71.7)	
Tumor size (cm)	3.0 ± 1.6	2.9 ± 1.6	0.527*
Extrathyroidal extension			
Negative	167 (71.7)	161 (66.0)	0.180†
Positive	66 (28.3)	83 (34.0)	
Multifocality			
Negative	136 (56.4)	126 (52.1)	0.336†
Positive	105 (43.6)	116 (47.9)	
T-stage			
T1	72 (29.3)	70 (28.6)	0.473†
T2	84 (34.1)	77 (31.4)	
T3	81 (32.9)	85 (34.7)	
T4	9 (3.7)	13 (5.3)	
Regional lymph node			
N0	129 (60.0)	94 (40.7)	<0.001†
N1	86 (40.0)	137 (59.3)	
Distant metastasis			
M0	124 (96.9)	150 (96.8)	0.962†
M1	4 (3.1)	5 (3.2)	
TNM stage group			
I	138 (56.3)	142 (57.7)	0.618†
II	33 (13.5)	17 (6.9)	
III	49 (20.0)	59 (24.0)	
IV	25 (10.2)	28 (11.4)	
BRAF V600E mutation			
Absent	157 (63.8)	97 (39.3)	<0.001†
Present	89 (36.2)	150 (60.7)	
TDS	0.39 ± 1.28	-0.43 ± 0.78	<0.001*

* P-values were calculated by Student's t-test. Data are expressed as means ± SD.

† P-values calculated by χ^2 test or linear-by-linear association.

Table 7. Univariate analysis of clinicopathological parameters and LOC100507661 expression according to the presence or absence of lymph node metastasis from the TCGA thyroid cancer database

	Lymph node metastasis		P-value
	Absent (N = 227), n (%)	Present (N = 226), n (%)	
LOC100507661 group			
< median level	129 (57.8)	86 (38.6)	<0.001†
≥ median level	94 (42.2)	137 (61.4)	
Age (yr), mean ± SD	49.0 ± 15.1	45.4 ± 15.9	0.016*
Gender (F/M)			
Male	53 (23.3)	71 (31.4)	0.054†
Female	174 (76.7)	155 (68.6)	
Tumor size (cm)	2.7 ± 1.5	3.2 ± 1.7	0.004*
Extrathyroidal extension			
Negative	168 (78.1)	124 (56.1)	<0.001†
Positive	47 (21.9)	97 (43.9)	
Multifocality			
Negative	128 (57.4)	108 (48.9)	0.072†
Positive	95 (42.6)	113 (51.1)	
T-stage			
T1	88 (38.8)	44 (19.6)	<0.001†
T2	75 (33.0)	67 (29.8)	
T3	60 (26.4)	96 (42.7)	
T4	4 (1.8)	18 (8.0)	
Distant metastasis			
M0	143 (97.9)	128 (97.0)	0.604†
M1	3 (2.1)	4 (3.0)	
TNM stage group			
I	139 (61.5)	114 (50.4)	<0.001†
II	40 (17.7)	2 (0.9)	
III	42 (18.6)	62 (27.4)	
IV	5 (2.2)	48 (21.2)	
BRAF V600E mutation			
Absent	127 (55.9)	107 (47.3)	0.067†
Present	100 (44.1)	119 (52.7)	
TDS	0.31 ± 1.18	-0.42 ± 0.96	<0.001*

* P-values were calculated by Student's t-test. Data are expressed as means ± SD.

† P-values calculated by χ^2 test or linear-by-linear association.

Table 8. Univariate analysis of clinicopathological parameters and LOC100507661 expression according to the presence or absence of the BRAF V600E mutation from the TCGA thyroid cancer database

	BRAF V600E mutation		P-value
	Absent (N =263), n (%)	Present (N = 240), n (%)	
LOC100507661 group			
< median level	157 (61.8)	89 (37.2)	<0.001†
≥ median level	97 (38.2)	150 (62.8)	
Age (yr), mean ± SD	46.8 ± 16.1	47.7 ± 15.5	0.510*
Gender (F/M)			
Male	68 (25.9)	67 (27.9)	0.602†
Female	195 (74.1)	173 (72.1)	
Tumor size (cm)	3.0 ± 1.5	2.9 ± 1.6	0.373*
Extrathyroidal extension			
Negative	190 (76.0)	143 (60.9)	<0.001†
Positive	60 (24.0)	92 (39.1)	
Multifocality			
Negative	139 (54.3)	127 (53.6)	0.874†
Positive	117 (45.7)	110 (46.4)	
T-stage			
T1	74 (28.2)	69 (28.9)	0.169†
T2	100 (38.2)	66 (27.6)	
T3	78 (29.8)	91 (38.1)	
T4	10 (3.8)	13 (5.4)	
Regional lymph node			
N0	127 (54.3)	100 (45.7)	0.067†
N1	107 (45.7)	119 (54.3)	
Distant metastasis			
M0	138 (97.2)	142 (96.6)	0.775†
M1	4 (2.8)	5 (3.4)	
TNM stage group			
I	153 (58.4)	131 (54.8)	0.122†
II	33 (12.6)	18 (7.5)	
III	51 (19.5)	60 (25.1)	
IV	25 (9.5)	30 (12.6)	
TDS	0.91 ± 0.99	-0.62 ± 0.78	<0.001*

* P-values were calculated by Student's t-test. Data are expressed as means ± SD.

† P-values calculated by χ^2 test or linear-by-linear association.

Table 9. Multivariate analysis of the association between lymph node metastasis and high LOC100507661 expression status from the TCGA thyroid cancer database

High LOC100507661	Lymph node metastasis		
	Odds ratio	95% CI	P-value
Model 1	2.071	1.410–3.041	<0.001
Model 2	1.889	1.177–3.032	0.008

Model 1. Adjusted for age and gender.

Model 2. Adjusted for age, gender, tumor size, extrathyroidal extension, multifocality, and BRAF V600E mutation.

Abbreviation: CI, confidence interval.

Table 10. Multivariate analysis of the association between the BRAF V600E mutation and high LOC100507661 expression from the TCGA thyroid cancer database

High LOC100507661	BRAF V600E mutation		
	Odds ratio	95% CI	P-value
Model 1	2.848	1.966–4.128	<0.001
Model 2	2.265	1.436–3.573	<0.001

Model 1. Adjusted for age and gender.

Model 2. Adjusted for age, gender, tumor size, extrathyroidal extension, multifocality, and lymph node metastasis.

Abbreviation: CI, confidence interval.

9. LOC100507661 is regulated by the BRAF signaling pathway

To investigate the mechanism of LOC100507661, we examined the relationship among LOC100507661 and major signaling pathways in thyroid cancer. To investigate whether the upregulation of LOC100507661 has an effect on BRAF signaling pathway, the expression levels of total and phosphorylated ERK, AKT were measured by western blot. None of these molecules changed in TPC1-7661 and 8505C-7661 cells (Fig. 8A, 8B).

Therefore, we tested whether the BRAF signaling modulation affect on LOC100507661 expression in 8505C cells. We expected that LOC100507661 expression will be downregulated by BRAF signaling inhibition. Unexpectedly, LOC100507661 expression was upregulated in response to MEK inhibitors (U0126, PD98059) and ERK direct inhibitor (SCH772984) (Fig. 8C, 8D). These results suggest that LOC100507661 is regulated by the BRAF signaling pathway.

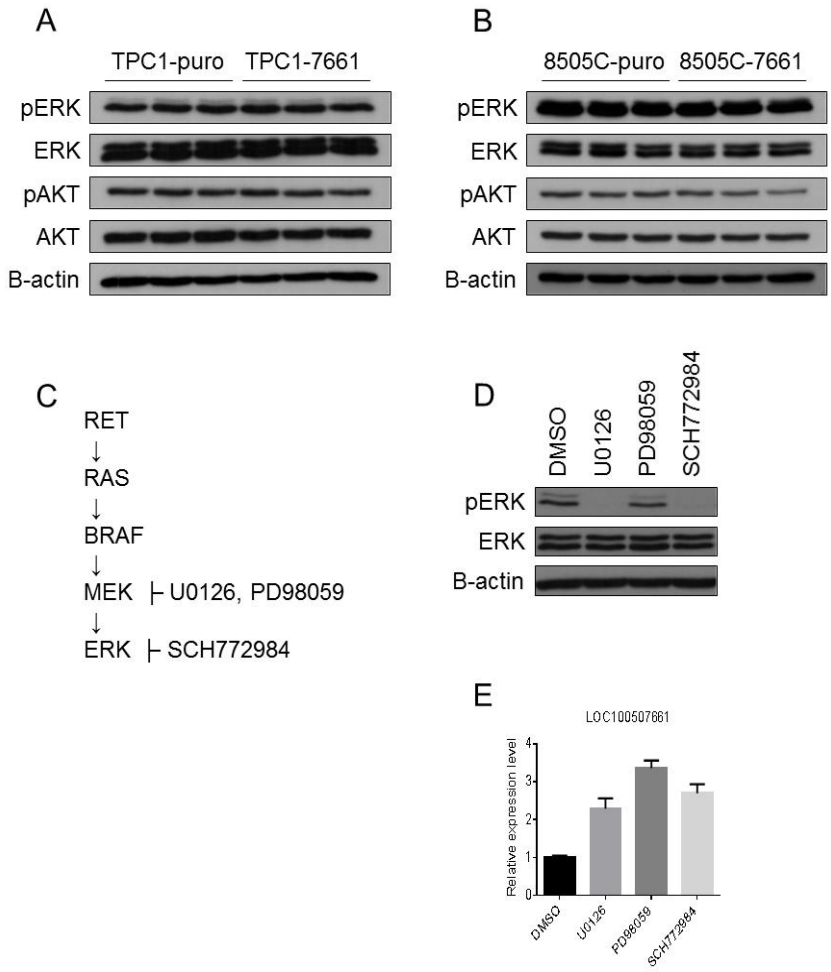

Figure 8. LOC100507661 is regulated by the BRAF signaling pathway. (A) Western blot with antibodies against pERK, ERK, pAKT and AKT are shown in TPC1-puro and TPC1-7661 cells. (B) Western blot with antibodies against pERK, ERK, pAKT and AKT are shown in 8505C-puro and 8505C-7661 cells. (C) Schematic representation of the BRAF signaling pathway. (D) Western blot with antibodies against pERK, ERK are shown after drug treatment. 8505C cells were treated with 10uM of U0126, 20uM of PD98059, and 1uM of SCH772984 for 24 hr. (E) Relative expression level of LOC100507661 after drug treatment determined by real-time PCR.

10. RAF inhibitor induces expression of LOC100507661 and activation of HER3 in 8505C cells

Because BRAF signaling inhibition upregulated LOC100507661 expression, not downregulated, we considered the possibility that LOC100507661 is related to resistance to BRAF V600E inhibition. We treated 8505C cells with the RAF inhibitor (PLX4720). PLX4720 upregulated LOC100507661 expression like U0126 (Fig. 9A, 9C). U0126 and PLX4720 also upregulated transcription, and expression of HER3 which is related to possible resistance mechanisms to BRAF V600E inhibition in thyroid cancer (Fig. 9A, 9B).

We obtained gene expression profiles at 0, 4, 8, 24, and 48 hr after addition of PLX4720 to 8505C cells, and identified upregulation of HER3 is earlier than upregulation of LOC100507661 (Fig. 9D, 9E, 9F).

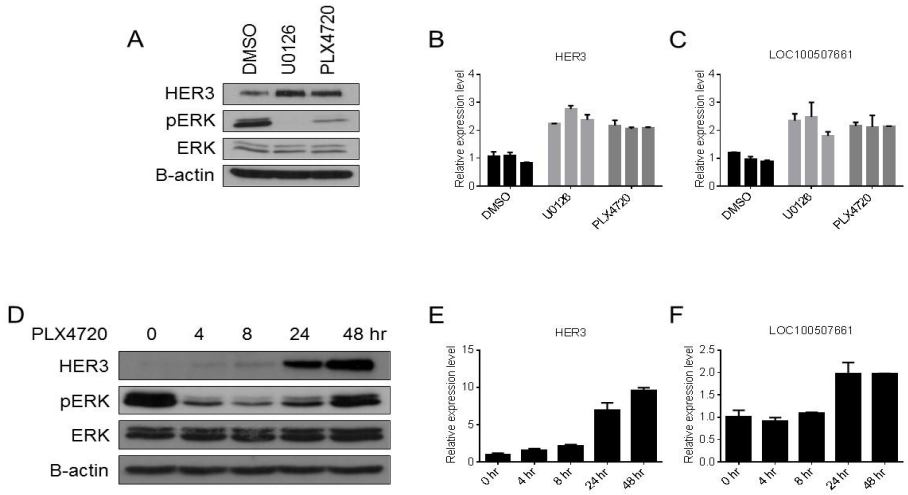

Figure 9. RAF inhibitor induces expression of LOC100507661 and activation of HER3 in 8505C cells. (A) Western blot with antibodies against HER3, pERK and ERK are shown after drug treatment. 8505C cells were treated with 10uM of U0126 and 1uM of PLX4720 for 24 hr. (B) Relative expression level of HER3 after drug treatment determined by real-time PCR. (C) Relative expression level of LOC100507661 after drug treatment determined by real-time PCR. (D) Western blot with antibodies against HER3, pERK and ERK are shown at 0, 4, 8, 24, and 48 hr after addition of PLX4720 to 8505C cells. (E, F) Relative expression level of HER3 and LOC100507661 after addition of PLX4720 determined by real-time PCR.

11. Transfection of siBRAF or pCMV-MEK1-DD affect HER3 gene transcription and expression of LOC100507661 in 8505C cells

Many drugs may affect more than one gene. We cannot exclude the possibility that effect of drugs was due to off-target effects. We used siBRAF to direct inhibition of BRAF. Treatment of 8505C cells with siBRAF resulted HER3 activation and upregulation of LOC100507661 (Fig. 10A, 10B, 10C).

By contrast, treatment of 8505C cells with pCMV-MEK1-DD (constitutively active form) decreases HER3 gene transcription and expression of LOC100507661 (Fig. 10D, 10E, 10F).

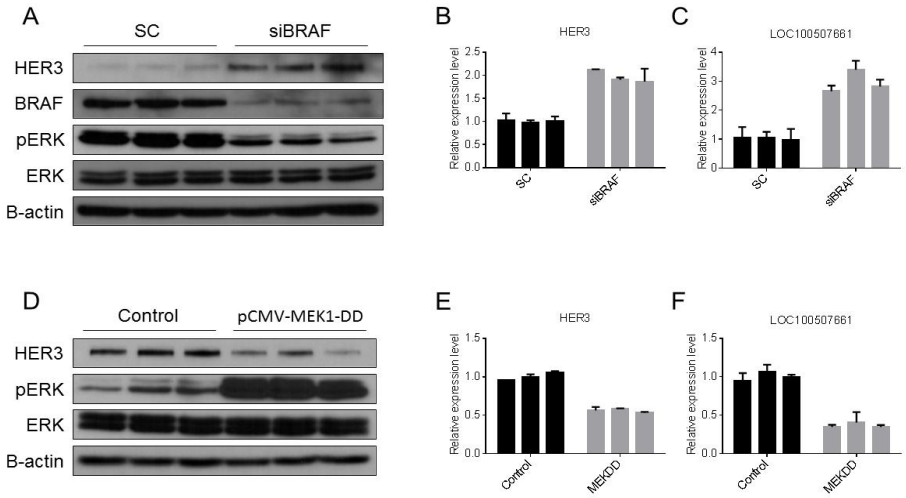

Figure 10. Transfection of siBRAF or pCMV-MEK1-DD affect HER3 gene transcription and expression of LOC100507661 in 8505C cells. (A) Western blot with antibodies against HER3, BRAF, pERK and ERK are shown at 48 hr after transfection of siBRAF. (B, C) Relative expression level of HER3 and LOC100507661 after transfection of siBRAF. (D) Western blot with antibodies against HER3, pERK and ERK are shown at 72 hr after transfection of pCMV-MEK1-DD. (E, F) Relative expression level of HER3 and LOC100507661 after transfection of pCMV-MEK1-DD.

12. Knockdown of HER3 downregulated LOC100507661 expression

To address the relationship between HER3 and LOC100507661 directly, siRNA was used to inhibit HER3 expression. siHER3-1 and siHER3-2 was found to have high silencing efficiency and downregulated LOC100507661 expression (Fig. 11A, 11B, 11C). These data suggest that LOC100507661 expression is regulated by HER3 in thyroid cancer cell line.

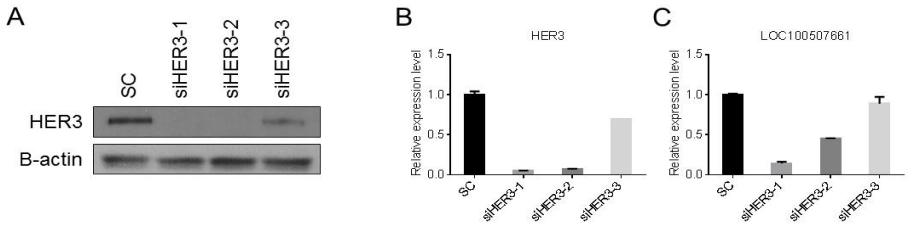

Figure 11. Knockdown of HER3 downregulated LOC100507661 expression. (A) Western blot with antibodies against HER3 are shown at 48 hr after transfection of siHER3-1, 2, 3. (B, C) Relative expression level of HER3 and LOC100507661 after transfection of siHER3-1, 2, 3.

13. Correlation between LOC100507661 expression and HER3 expression from the TCGA thyroid cancer database

We analyzed merged data from The Atlas of Noncoding RNAs in Cancer (TANRIC) and The Cancer Genome Atlas (TCGA). HER3 expression is higher in thyroid cancer tissue than normal tissue (Fig. 12A, 12B). As our previous data, the expression levels of LOC100507661 were higher in the BRAF V600E mutant group than in the wild group (Fig. 12C). HER3 levels were also higher in the BRAF V600E mutant group than in the wild group (Fig. 12D). LOC100507661 expressions were correlated with HER3 expressions ($r = 0.3242$, $P < 0.0001$) (Fig. 12E). These data support our cell line results that LOC100507661 expression is regulated by HER3 activation.

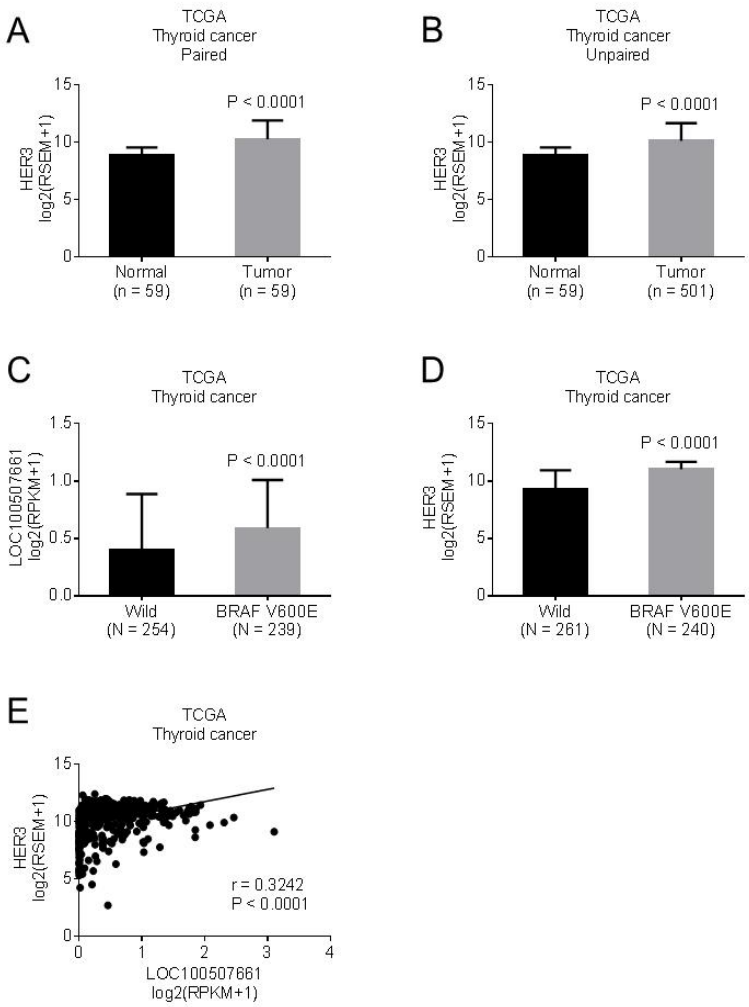

Figure 12. Correlation between LOC100507661 expression and HER3 expression from the TCGA thyroid cancer database. (A, B) LOC100507661 levels in thyroid cancer tissue and normal tissue. (C) LOC100507661 levels in the BRAF V600E mutant group and in the wild group. (D) HER3 levels in the BRAF V600E mutant group and in the wild group. (E) Correlation between LOC100507661 expression and HER3 expression.

IV. DISCUSSION

Thyroid cancer is the most common endocrine malignancy.[27] The prognosis of patients with differentiated thyroid cancer (DTC) is generally favorable because surgery, with or without radioactive iodine therapy, can induce complete remission in most cases.[28] However, the current diagnostic and therapeutic strategy is not completely effective in all cases. Although recent advances in our understanding of thyroid carcinogenesis revealed that molecular markers such as BRAF V600E and TERT promoter mutation have diagnostic and therapeutic implications, fine-needle aspiration cytology yields a significant proportion of indeterminate results, e.g., atypia of undetermined significance/follicular lesion of undetermined significance (AUS/FLUS).[29,30] In addition, 10–15% of patients with DTC present with refractory or recurrent thyroid cancers. Commercially available kinase inhibitors such as sorafenib can be used in such patients, but complete remission is not frequently achieved.[31] In light of these observations, new biomarkers are still needed to overcome diagnostic and therapeutic obstacles in a subset of patients with DTC.[32-34]

Recent studies have suggested that lncRNAs play causal roles in carcinogenesis and are involved in prognosis, metastasis, and recurrence in various types of cancer.[5] However, our knowledge of the role of lncRNAs remains limited. The first objective of this study was to discover novel lncRNA genes with oncogenic activity in thyroid cancer. To achieve this goal, we used a database of lncRNA-containing SCNAs in multiple types of tumors and selected three potential candidate genes (CTD-3080P12.3, LOC100507661, and TERC) for further analysis.[23] TERC encodes the RNA component of the telomerase complex, which extends telomeres. Although upregulation of TERT, a protein component of telomerase, is associated with aggressiveness in thyroid cancer, TERC was downregulated in thyroid cancer tissue.[35] No functional information was available regarding CTD-3080P12.3 and LOC100507661, but because LOC100507661 was

strikingly upregulated (20–100-fold relative to normal tissues), we decided to further investigate its role in thyroid cancer. Consistent with our real-time PCR data, recently deposited the TCGA thyroid cancer database and the GEO dataset (GSE66783) also supports our finding that LOC100507661 is upregulated in thyroid cancer.

In general, functional studies of lncRNAs are challenging because these molecules exert their cell biological functions via diverse mechanisms.[4] In this study, we attempted to knockdown LOC100507661 using shRNA and GapmeR technology, but failed to achieve efficient silencing. At least two phenomena might explain the low efficiency of knockdown against LOC100507661. First, as shown in Fig. 4C, LOC100507661 is (like most lncRNAs) exclusively localized in the nucleus. In general, nuclear lncRNAs cannot be depleted by shRNA unless they shuttle between the nucleus and cytosol. Second, the secondary structure of the lncRNA might prevent shRNA or GapmeR from accessing the target region. As shown in Fig. 2B, the base pairing of exon 1 and 2 might generate such an inhibitory secondary structure; however, this hypothesis is speculative.

This study using a stable overexpression system clearly revealed that LOC100507661 can promote cell proliferation, migration, and invasion. Consistent with our in vitro data, lymph node metastasis and BRAF V600E mutations were more frequent in patients with PTCs with high LOC100507661 expression. Remarkably, expression of LOC100507661 was also detected in metastatic lymph nodes, indicating that metastatic tumor cells might also require LOC100507661 for their survival, proliferation, migration, or invasion. Strategies for therapeutic manipulation of lncRNAs, such as ‘antagoNAT’ (natural antisense transcripts), are currently being developed.[36]

LOC100507661 expression is elevated in thyroid cancer and it promotes tumor aggressiveness in this study. Therefore, we examined the relationship among LOC100507661 and major signaling pathways in thyroid cancer to investigate the mechanism of LOC100507661. Overexpression of LOC100507661 did not change

BRAF signaling pathway in thyroid cancer cell lines. Unexpectedly, we showed that inhibition of BRAF signaling by MEK and ERK inhibitors upregulated LOC100507661 expression. To verify these findings, siBRAF or constitutively active MEK plasmid was transfected into the 8505C cells. We found that BRAF signaling pathway negatively regulate LOC100507661 expression. These results demonstrated that LOC100507661 expression is not directly modulated by BRAF V600E mutations. It may be RAF like tumor has high LOC100507661 expression.[18] BRAF-RAS score (BRS) and thyroid differentiation score (TDS) are highly correlated across all tumors, and our study showed that TDS was negatively associated with high LOC100507661 expression. Elevated HER3 in thyroid cancer especially in BRAF V600E mutant group can explain it.[37-40]

One of possible resistance mechanisms to BRAF V600E inhibition in thyroid cancer is mediated by increased upstream signaling and activation of molecules providing signaling alternatives to BRAF V600E.[41] In our study, RAF inhibitor transiently inhibits the ERK pathway and upregulated HER3 transcription. LOC100507661 was clearly induced by RAF inhibitor or siBRAF correlated with HER3, and siHER3 inhibited LOC100507661 expression. These observations suggested that LCO100507661 could be a downstream target gene of HER3. Previous study report that the majority of BRAF mutant thyroid cancer cell lines are insensitive to the growth inhibitory effects of PLX4032, and that is largely due to a feedback induced ligand dependent activation of HER2/HER3 signaling.[42] Therefore, a potential mechanism for LOC100507661 expression is, in part, through HER3 regulation. And we can considered the possibility that LOC100507661 is related to resistance to BRAF V600E inhibition, but more studies are needed.

Compatible to our cell line study, the analysis using merged data from TANRIC and TCGA indicated that that HER3 was elevated in thyroid cancer and LOC100507661 expressions had positive correlation with HER3 expressions in thyroid cancer. It is known that the increase in expression of HER3 is due to the

activation of gene transcription.[42] This correlation also supports that LOC100507661 expression is regulated by HER3 activation. Further mechanistic explanations of HER3-LOC100507661 signaling pathway to develop new drug targets for invasive or metastatic thyroid cancers are needed.

An unresolved problem in the present study was our failure to knockdown LOC100507661. Additional structural or functional studies of LOC100507661 are needed. We also plan to investigate LOC100507661 silencing technology from the standpoint of therapeutic applications.

V. CONCLUSION

In conclusion, LOC100507661 expression is elevated in human PTC and metastatic lymph nodes, and high expression of LOC100507661 is correlated with lymph node metastasis and BRAF V600E mutations. In vitro, LOC100507661 promotes tumor cell proliferation, migration, and invasion. LOC100507661 expression was regulated by HER3 in thyroid cancer cell line. These findings suggest that LOC100507661 represents a potential biomarker and therapeutic target in thyroid cancer.

REFERENCES

1. International Human Genome Sequencing C. Finishing the euchromatic sequence of the human genome. Nature 2004;431:931-45.
2. Kim VN, Han J, Siomi MC. Biogenesis of small RNAs in animals. Nat Rev Mol Cell Biol 2009;10:126-39.
3. Derrien T, Johnson R, Bussotti G, Tanzer A, Djebali S, Tilgner H, et al. The GENCODE v7 catalog of human long noncoding RNAs: analysis of their gene structure, evolution, and expression. Genome Res 2012;22:1775-89.
4. Wang KC, Chang HY. Molecular mechanisms of long noncoding RNAs. Mol Cell 2011;43:904-14.
5. Prensner JR, Chinnaiyan AM. The emergence of lncRNAs in cancer biology. Cancer Discov 2011;1:391-407.
6. Venkatesh T, Suresh PS, Tsutsumi R. Non-coding RNAs: Functions and applications in endocrine-related cancer. Mol Cell Endocrinol 2015;416:88-96.
7. Barsyte-Lovejoy D, Lau SK, Boutros PC, Khosravi F, Jurisica I, Andrulis IL, et al. The c-Myc oncogene directly induces the H19 noncoding RNA by allele-specific binding to potentiate tumorigenesis. Cancer Res 2006;66:5330-7.
8. Chunharojrith P, Nakayama Y, Jiang X, Kery RE, Ma J, De La Hoz Ulloa CS, et al. Tumor suppression by MEG3 lncRNA in a human pituitary tumor derived cell line. Mol Cell Endocrinol 2015;416:27-35.
9. Ji P, Diederichs S, Wang W, Boing S, Metzger R, Schneider PM, et al. MALAT-1, a novel noncoding RNA, and thymosin beta4 predict metastasis and survival in early-stage non-small cell lung cancer. Oncogene 2003;22:8031-41.
10. Rinn JL, Kertesz M, Wang JK, Squazzo SL, Xu X, Brugmann SA, et al.

Functional demarcation of active and silent chromatin domains in human HOX loci by noncoding RNAs. Cell 2007;129:1311-23.

11. Tripathi V, Shen Z, Chakraborty A, Giri S, Freier SM, Wu X, et al. Long noncoding RNA MALAT1 controls cell cycle progression by regulating the expression of oncogenic transcription factor B-MYB. PLoS Genet 2013;9:e1003368.
12. Yoon H, He H, Nagy R, Davuluri R, Suster S, Schoenberg D, et al. Identification of a novel noncoding RNA gene, NAMA, that is downregulated in papillary thyroid carcinoma with BRAF mutation and associated with growth arrest. Int J Cancer 2007;121:767-75.
13. He H, Li W, Liyanarachchi S, Jendrzejewski J, Srinivas M, Davuluri RV, et al. Genetic predisposition to papillary thyroid carcinoma: involvement of FOXE1, TSHR, and a novel lincRNA gene, PTCSC2. J Clin Endocrinol Metab 2015;100:E164-72.
14. He H, Nagy R, Liyanarachchi S, Jiao H, Li W, Suster S, et al. A susceptibility locus for papillary thyroid carcinoma on chromosome 8q24. Cancer Res 2009;69:625-31.
15. Jendrzejewski J, He H, Radomska HS, Li W, Tomsic J, Liyanarachchi S, et al. The polymorphism rs944289 predisposes to papillary thyroid carcinoma through a large intergenic noncoding RNA gene of tumor suppressor type. Proc Natl Acad Sci U S A 2012;109:8646-51.
16. Jendrzejewski J, Thomas A, Liyanarachchi S, Eiterman A, Tomsic J, He H, et al. PTCSC3 Is Involved in Papillary Thyroid Carcinoma Development by Modulating S100A4 Gene Expression. J Clin Endocrinol Metab 2015;100:E1370-7.
17. Wang Y, Guo Q, Zhao Y, Chen J, Wang S, Hu J, et al. BRAF-activated long non-coding RNA contributes to cell proliferation and activates autophagy in papillary thyroid carcinoma. Oncol Lett 2014;8:1947-52.
18. Cancer Genome Atlas Research N. Integrated genomic characterization

of papillary thyroid carcinoma. Cell 2014;159:676-90.

19. Cancer Genome Atlas Research N, Weinstein JN, Collisson EA, Mills GB, Shaw KR, Ozenberger BA, et al. The Cancer Genome Atlas Pan-Cancer analysis project. Nat Genet 2013;45:1113-20.
20. Li J, Han L, Roebuck P, Diao L, Liu L, Yuan Y, et al. TANRIC: An Interactive Open Platform to Explore the Function of lncRNAs in Cancer. Cancer Res 2015;75:3728-37.
21. Fusco D, Accornero N, Lavoie B, Shenoy SM, Blanchard JM, Singer RH, et al. Single mRNA molecules demonstrate probabilistic movement in living mammalian cells. Curr Biol 2003;13:161-7.
22. Kim SJ, Choi IJ, Cheong TC, Lee SJ, Lotan R, Park SH, et al. Galectin-3 increases gastric cancer cell motility by up-regulating fascin-1 expression. Gastroenterology 2010;138:1035-45 e1-2.
23. Hu X, Feng Y, Zhang D, Zhao SD, Hu Z, Greshock J, et al. A functional genomic approach identifies FAL1 as an oncogenic long noncoding RNA that associates with BMI1 and represses p21 expression in cancer. Cancer Cell 2014;26:344-57.
24. Sato K, Hamada M, Asai K, Mituyama T. CENTROIDFOLD: a web server for RNA secondary structure prediction. Nucleic Acids Res 2009;37:W277-80.
25. Mercer TR, Mattick JS. Structure and function of long noncoding RNAs in epigenetic regulation. Nat Struct Mol Biol 2013;20:300-7.
26. Park JH, Lee KS, Bae K-S, Kang SJ. Regional Lymph Node Metastasis in Papillary Thyroid Cancer. J Korean Thyroid Assoc 2014;7:129-35.
27. Davies L, Welch HG. Increasing incidence of thyroid cancer in the United States, 1973-2002. JAMA 2006;295:2164-7.
28. Haugen BR, Alexander EK, Bible KC, Doherty GM, Mandel SJ, Nikiforov YE, et al. 2015 American Thyroid Association Management Guidelines for Adult Patients with Thyroid Nodules and Differentiated

Thyroid Cancer: The American Thyroid Association Guidelines Task Force on Thyroid Nodules and Differentiated Thyroid Cancer. Thyroid 2016;26:1-133.

29. Cohen Y, Xing M, Mambo E, Guo Z, Wu G, Trink B, et al. BRAF mutation in papillary thyroid carcinoma. J Natl Cancer Inst 2003;95:625-7.
30. Nikiforov YE, Carty SE, Chiosea SI, Coyne C, Duvvuri U, Ferris RL, et al. Impact of the Multi-Gene ThyroSeq Next-Generation Sequencing Assay on Cancer Diagnosis in Thyroid Nodules with Atypia of Undetermined Significance/Follicular Lesion of Undetermined Significance Cytology. Thyroid 2015;25:1217-23.
31. Perez CA, Santos ES, Arango BA, Raez LE, Cohen EE. Novel molecular targeted therapies for refractory thyroid cancer. Head Neck 2012;34:736-45.
32. Fagin JA. How thyroid tumors start and why it matters: kinase mutants as targets for solid cancer pharmacotherapy. J Endocrinol 2004;183:249-56.
33. Hwang TS. Molecular Diagnosis for Cytologically Indeterminate Thyroid Nodules. Int J Thyroidol 2015;8:153-60.
34. Kim JG. Molecular pathogenesis and targeted therapies in well-differentiated thyroid carcinoma. Endocrinol Metab (Seoul) 2014;29:211-6.
35. Liu X, Bishop J, Shan Y, Pai S, Liu D, Murugan AK, et al. Highly prevalent TERT promoter mutations in aggressive thyroid cancers. Endocr Relat Cancer 2013;20:603-10.
36. Wahlestedt C. Targeting long non-coding RNA to therapeutically upregulate gene expression. Nat Rev Drug Discov 2013;12:433-46.
37. Kato S, Kobayashi T, Yamada K, Nishii K, Sawada H, Ishiguro H, et al. Expression of erbB receptors mRNA in thyroid tissues. Biochim

Biophys Acta 2004;1673:194-200.

38. Kim HS, Kim DH, Kim JY, Jeoung NH, Lee IK, Bong JG, et al. Microarray analysis of papillary thyroid cancers in Korean. Korean J Intern Med 2010;25:399-407.

39. Wiseman SM, Griffith OL, Melck A, Masoudi H, Gown A, Nabi IR, et al. Evaluation of type 1 growth factor receptor family expression in benign and malignant thyroid lesions. Am J Surg 2008;195:667-73; discussion 73.

40. Schulten HJ, Alotibi R, Al-Ahmadi A, Ata M, Karim S, Huwait E, et al. Effect of BRAF mutational status on expression profiles in conventional papillary thyroid carcinomas. BMC Genomics 2015;16 Suppl 1:S6.

41. Hanly EK, Tuli NY, Bednarczyk RB, Suriano R, Geliebter J, Moscatello AL, et al. Hyperactive ERK and persistent mTOR signaling characterize vemurafenib resistance in papillary thyroid cancer cells. Oncotarget 2016;7:8676-87.

42. Montero-Conde C, Ruiz-Llorente S, Dominguez JM, Knauf JA, Viale A, Sherman EJ, et al. Relief of feedback inhibition of HER3 transcription by RAF and MEK inhibitors attenuates their antitumor effects in BRAF-mutant thyroid carcinomas. Cancer Discov 2013;3:520-33.

ABSTRACT(IN KOREAN)

갑상선암에서 발암활성을 가지는 Long Noncoding RNA LOC100507661

<지도교수 김경섭>

연세대학교 대학원 의과학과

김다함

최근 차세대 염기서열 분석법의 발전으로 다양한 long noncoding RNAs (lncRNAs)가 밝혀지고 있다. 그러나 lncRNAs에 대한 연구는 아직까지 초기 단계로 생물학적 기능이나 임상적 의미에 대해서는 잘 알려져 있지 않다. 갑상선암에서 lncRNAs의 역할을 확인하기 위해 본 연구에서는 12가지 암에서 2,394개의 SNP 분석을 시행한 연구를 바탕으로 암 발생에 관여할 것으로 기대되는 56개의 lncRNAs를 확인하였다. 그리고 NCBI와 Ensembl에서 확인된 시퀀스 정보 바탕으로 분석을 진행할 세가지 후보 lncRNAs를 선정하였다. 그 중 LOC100507661은 갑상선암 조직에서 주변의 정상 갑상선 조직에서보다 발현이 높게 증가되어 있었다. LOC100507661은 TPC1, BCPAP, C643, 그리고 8505C와 같은 유두상 갑상선암 세포주나 미분화 갑상선암 세포주에서 높게 발현이 되나, 여포상 갑상선암 세포주인 FTC133에서는 거의 발현이 되지 않았다.

LOC100507661을 지속적으로 과발현시킨 갑상선암 세포주에서 세포의 증식, 이동, 그리고 침입이 증가하였다. 갑상선암의 림프절 전이와 BRAF V600E 변이는 LOC100507661의 발현이 높은 환자군에서 더 많이 나타났다. 감상선암 세포주에서 LOC100507661의 발현은 HER3에 의해 조절되었다. 본 연구는 갑상선암에서 LOC100507661의 발현이 증가하며 갑상선암의 암화 과정에 중요한 역할을 한다는 것을 보여주었다. 앞으로 더 많은 연구가 필요하겠지만, LOC100507661과 같은 lncRNAs는 갑상선암에 있어 잠재적인 생물학적 지표와 치료 표적자가 될 수 있을 것으로 기대된다.

핵심되는 말 : long noncoding RNA, LOC100507661, 갑상선암, 발암

PUBLICATION LIST

1. Kim D, Lee WK, Jeong S, Seol MY, Kim H, Kim KS, et al. Upregulation of long noncoding RNA LOC100507661 promotes tumor aggressiveness in thyroid cancer. Mol Cell Endocrinol 2016;431:36-45.